URSI - RCRS 2022, IIT (Indore), India, 1 - 4 December, 2022

Biological Liquid Monitoring using Microwave Resonator

Shalini Patel[(1)], Soumyadeep Das* [(2)], Debasis Mitra[(3)], Subhasis Sarkar[(4)], Chaitali Koley[(5)]
(1) NIT Mizoram, India, 796012
(2) Techno India university Kolkata, India, 700091
(3) IIEST Shibpur, Howrah, West Bengal,India, 711103
(4) College of Medicine and Sagore Datta hospital Kamarhati, Kolkata, India, 700058
(5) NIT Mizoram, India, 796012

***Abstract*—For dielectric characterisation of liquids, a novel microwave sensor is designed on the concept of metamaterial (MTM) by using complementary split ring resonator (CSRR). This work describes an MTM based high-sensitivity microwave sensor with a PDMS channel that can be used for any kind of liquid detection and in a number of biomedical applications. On the ground plane of a dielectric substrate, three CSRRs with squared shapes are engraved. A planar microstrip-line (MTL) carved on the substrate's bottom side generates a time-varying electric field that is connected to the sensor cells to stimulate them. The sensor has been built on a Rogers RT6002 dielectric substrate. The sensitivity of the proposed sensor is demonstrated in laboratory tests with a variety of liquid samples using a Vector Network Analyzer (VNA) setup, where the frequency is different for different dielectric constants. The designed sensor has a remarkable ability to detect minor dielectric variations, in addition to having other beneficial qualities including compact size, easy manufacture, cheap, nonionizing nature, and no risk to human health. The use of the proposed sensor along with additional microwave components for non-invasive disease diagnosis may be encouraged by such crucial properties.**

Keywords—complementary split ring resonator (CSRR), liquid sensing, dielectric constant, microstrip line (MTL), polydimethylsiloxane (PDMS)

1. Introduction

TODAY'S technology has created a growing demand for compact, inexpensive, highly sensitive, selective, and long-lasting sensing devices that can be used in a number of healthcare and biological applications [1]. Microwave technology is highly demanding in addition to existing high frequency technologies since it is efficient, low cost, nonionizing, portable, and pleasant. The demand for continuous monitoring and early diagnosis in the biomedical arena is growing by the day. X-ray and CT scan are two procedures that cannot continuously monitor patients and emit dangerous radiation. Furthermore, MRI is an expensive and time-consuming diagnostic procedure [2]. Microwaves poses low risk to the human body in biomedical applications and are low-cost equipment. Because of its minimal health risk applicability, microwave techniques for liquid sensing are in high demand these days. The objective is to offer efficient and straightforward sensing systems that are simple to tune at variable frequency to meet application needs. Recently, in the field of microwave frequency-based antennas and sensors, a new type of metamaterial known as MTMs, have been emerged with a lot of applications [3].

Antenna based on the concept of metamaterial structure has been used here because of its small size and high performance. MTM's have some unique properties like, negative effective permittivity, negative effective permeability, negative refraction index, and reverse wave propagation [8]. A SRR and a CSRR were originally used to achieve these special qualities. Later, microwave sensors for measuring thickness, relative humidity, permittivity, and permeability were made using these artificial structures [15], [16], and [17]. Because they combine the accuracy of conventional huge sensors with a smaller electrical size, small electrically sized MTL based sensors like the SRR and its CSRR are more suited for usage in sensing applications [3]. SRR and CSRR have many applications such as miniaturisation, simple fabrication, easily integration, and highly sensitive. They've been used in a variety of dielectric characterisation, bimolecular sensing, and microfluidic sensing applications [4].

Compact size, high sensitivity, low cost, and high accuracy are the key advantages of SRR and CSRR-based sensors. The planar microwave sensor's performance is influenced by the resonant structure and the hosting transmission line [5]. In this work, the sensor was tested using a variety of liquids. The sensors must be highly sensitive and potentially safe to use in order to precisely detect the various liquid volumes in such circumstances. In this work, the liquid samples are arranged parallel to the sensor surface on the polydimethylsiloxane (PDMS), allowing for fast investigation of liquid sample dielectric characteristics at microwave frequencies.

The ability to use samples across a PDMS channel is another significant aspect of the proposed sensor. The sensor is reusable, small, inexpensive, and easy to manufacture. The sensor has effectively detected various frequencies for different types of liquids with different dielectric constants, as tested by laboratory experiments.
The designed microfluidic sensor in this study is intended to both detect loaded liquid and track the varying dielectric characteristics of different liquids that are included in the PDMS channel. Basically, PDMS is a channel that is used in biological applications [6], we can hold liquids in PDMS, and a sensor allows us to detect any type of liquid. Due to its great mechanical resistance, optical transparency, chemical inertness, biocompatibility, and non-toxicity, the latter has been manufactured with the appropriate dimensions using PDMS [3] & [8]. To increase detection sensitivity, at the ground plane of the CSRR sensing components the sensitivity is very high so the channel has been placed at this region. Using a suitable VNA setup, the manufactured prototype has been tested for detecting a variety of liquid samples, which includes distilled water, a human mimicking model, and glycerol. This has been done by monitoring the frequency fluctuations of the resonances that are produced in the transmission and reflection scattering responses. The proposed low-cost, easily manufacture, and high sensitive microwave sensor for liquid detection applications has shown significant promise in experimental testing.
Section II describes the proposed sensor design, theoretical investigation, numerical analysis, and production procedures. Section III discusses the fluid in-lab tests and findings, as well as the performance analysis. Finally, the work's conclusion and the future scope are described in part IV.

2. Design of Sensor and Theoratical Study

A. Design and Specifications of proposed sensor

The metamaterial technology has been implemented in the sensor construction, as shown in fig. 1, three square shaped CSRRs in the dimensions of width W, thickness h, and length L has been printed on the top of the dielectric substrate. The distance from the first cell and input port is D1. CSRR cells are geographically separated by D2 distance ranges between cell boundaries. The three squared ring loops that make up the triplet split-rings each have a gap "g." The ends of each ring's loop meet in a split gap "s" metal slot. When the sensor is loaded symmetrically, a two-port feeding line MTL is installed on the bottom face of the dielectric substrate (cross section Lline × Wline) to excite the resonating cells from a linked RF power supply and achieve the broadband response.
Each CSRR cell's etched dielectric slits contain charges and currents that the microstrip structure stimulates, creating inductances and capacitances that store oscillating electric and magnetic energy. At a particular frequency, a CSRR sensor displays a bandgap resonance, when both the energies are balanced. When used to detect lossy dielectrics, the CSRR sensor's bandgap response can be affected by a number of design elements, such as resonance frequency, depth, and q - factor (i.e. liquid samples).
The resonance profile has been derived from the physical parameters, substrate requirements, and shape of each CSRR cell in the integrated structure. These parameters include the lengths of the external, internal, and middle squares (a, b, and c), the coupling gap (g), the ring width (r), the split gap (s), as well as the distances D1 and D2 that, respectively, correspond to the input and even in MTL delays. The proposed structure is created, and its geometrical parameters are established using the CST studio 2019 simulator, to intensify the resonance, the coupled electric fields within the permittivity sensing region. As a result, there is an improvement in sensitivity that can detect modifications to the dielectric characteristics of loaded liquid samples.

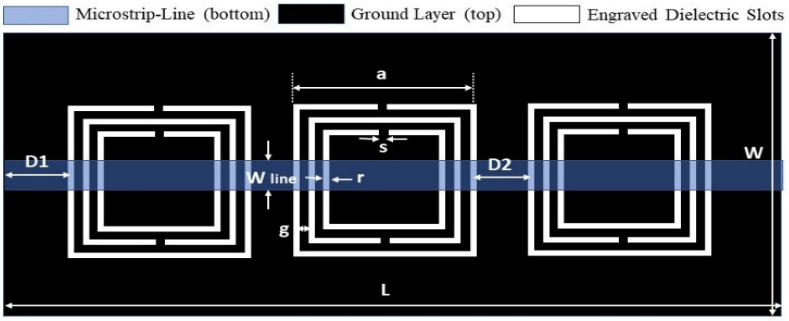

Figure 1. A Metamaterial CSRR cell (top view). On the bottom of the substrate, MTL is patterned.

On a Rogers RT6002 substrate with dimensions of length L=51 mm, width W=30 mm, and dielectric constant=2.9, the CSRR elements are designed. The CSRR cells have been positioned so that the magnetic wall of their symmetry plane is orthogonal to the direction of propagation and the axis of the MTL strip is parallel to the axis of the MTL strip in order to enable fully electric resonance excitation with a time-varying electric field between the MTL and ground plane. The thickness of the substrate “h” has been taken as 0.8mm to limit the electric polarisation in the substrate and to increase the transmission response's reliance on the liquid permittivity.
As a result, each CSRR cell's external square has been constructed with an outer length of 11mm, a ring width r = 0.5mm, and a split gap, s = 0.1mm. With width of the ring is, r = 0.5mm and gap of each spilt is, s = 0.5mm, the outer length of a mid-

square is, a = 9 mm is built similarly. With the width of the ring r = 0.5 mm and the outer length of the inner most square is, a = 7mm is designed accordingly. The distance “g” is the gap between the exterior and interior squares.
The MTL has been built with a width Wline = 1.3mm to match the feeding ports' 50ohm input impedance and so avoids any transmission-line reflections. Table I lists all the parameters of the designed sensor, which results in an unloaded transmission resonance of around 1.5 to 1.6GHz.

Table I
Dimensional specifications of the proposed sensor (in mm)

a	s	g	r	h	D1	D2	Wline	Lline	W	L
11	0.1	0.5	0.5	0.8	9	9	1.3	30	51	30

B. Numerical Analysis of proposed CSRR
The rectangular resonator and capacitive plate of the CSRR generate an electric field across this gap during resonance, making the area inside and around the CSRR sensitive to dielectric changes. As a result, it is possible to examine a material's dielectric properties in this area of the CSRR. Fig. 2 shows the distribution of the electric field at the surface of the proposed sensor at its resonance frequency of 1.6GHz.

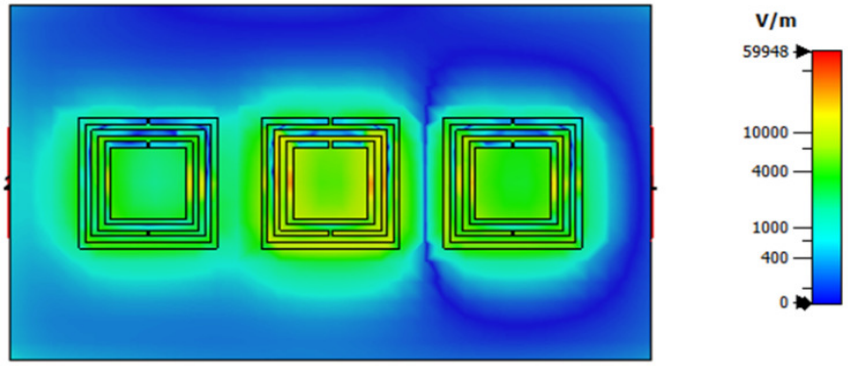

Figure 2. Proposed sensor’s electric field distribution.

The circuit model's resonance frequency can be defined as, [3]

$$fmc \propto \frac{1}{2\pi\sqrt{LR(CR+CC)}} \quad (1)$$

Where in equation (1), LR is the inductance added by the dielectric ring windings, CC is the coupling capacitance across the substrate, CR denotes the capacitance due to the metallic gaps "s" and space of each resonating cell is “g”. A sensor response is created that depends on the loaded liquid permittivity by lowering the geometrical parameters of each MTM cell to decrease the combined reactive elements LR and CR in every cell and lower the minimal transmission frequency "fmc." According to numerical analysis, the dielectric slit’s effective length is proportional to the cell length "a" and ring width "r," hence increasing "a" and "r" will result in an increase in LR and a drop in fmc.
The proposed sensor's performance is displayed in Fig. 3 together with simulated and measured results. First, as shown in Fig.3, both experimental and simulation investigations of the transmission coefficient response (S_{21}) of the structure in the normal condition (without PDMS) have been conducted.

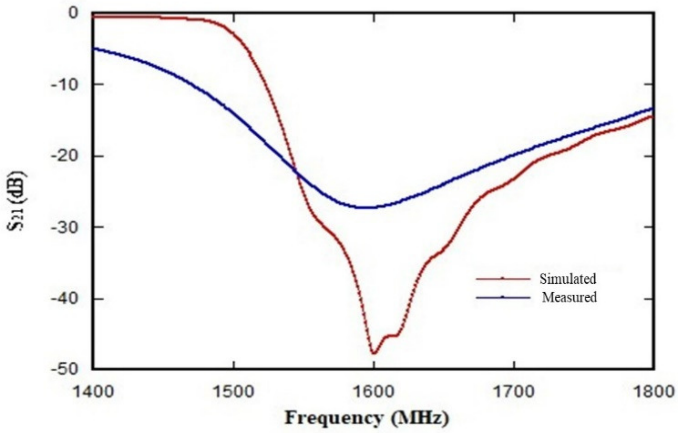

Figure 3. Simulated and measured result of the designed sensor.

Here sensor exhibits unloaded resonances around 1.6GHz, where the steeper resonance depth of CSRR is about −48dB in the simulated result while the measured result shows the resonance depth of −27.5dB. The consistency between experimental and simulation methods is good, with some minor variations caused by fabrication tolerances.

C. Prototype Fabrication

Using laser micromachining, a CSRR prototype has been created on a Rogers RT6002 substrate with a 35µm copper thickness. Each CSRR cell's outside and inner dielectric annular slits were cut using a laser on the substrate's top layer. as shown in Fig. 4(a). After aligning the laser beam with the fiducially markers, the MTL (51×1.3mm2) has been printed on the bottom layer. As indicated in Fig. 4(b), by connecting 50 SMA coaxial connectors to both ends of the MTL's, two ports have been added to the sensor.

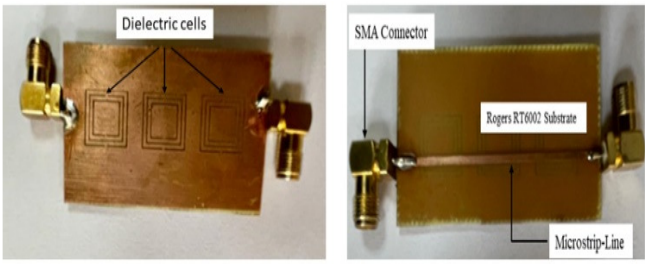

Figure 4. Fabricated CSRR sensor (a) Top view, and (b) Bottom view.

A typical soft lithography technique has been used to create the microfluidic channel, in which the sensor's architecture generate a complete sensing zone. The channel has been constructed with inner dimensions of the PDMS as 35×10×0.5mm^3 to be incorporated along the centre islands of the connected CSRRs to execute the sensing operation with improved sensitivity while using the least amount of liquid volume. The supporting PDMS has a wider width and length to ensure that the channel, having outside dimensions of PDMS as 48×25×3mm^3, completely aligned with the CSRR cells.

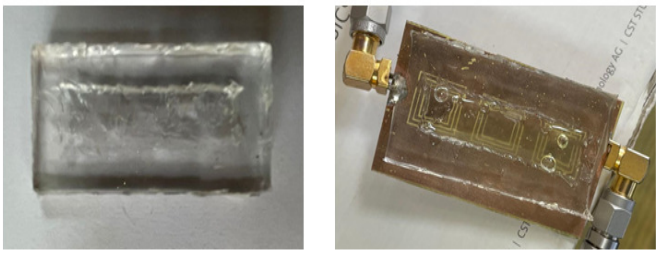

Figure 5. (a) PDMS (b) Layout of the final device

To make PDMS, a mixture of sylgard 184 silicon elastomer and its curing agent has been poured over the petri dish in the ratio of 10:1 and cured in a vacuum evaporator for 2 hours to remove all the bubbles, formed during the mixing process. After removing all the bubbles, it should be placed in a preheated oven at 80°C for 45 minutes to an hour to achieve the desired

hardness [1]. The resulting PDMS channel is formed which has been depicted in fig 5(a). It has been mounted on the top of the CSRR sensor with the detecting components precisely aligned to achieve the highest sensitivity while measuring the tested liquids, as presented in Fig. 5(b).

3. Performance Analysis and Experimental Measurement

A. Experimental Measurement

By connecting the sensor to the two ports of the VNA with coaxial cables in a stable configuration, as illustrated in Fig. 6, the sensor's performance is integrated with the PDMS channel which is tested and confirmed in lab [11]. To stimulate the microwave sensor and to observe the scattering response also known as transmission coefficient, (1-8 GHz) (S21), the Anristu S820E 40 GHz site master vectors Network Analyzer (VNA) has been used. A more robust machine learning model can be developed by increasing the frequency and amplitude of the multiple resonances produced by the S21 response. To offer more information, additional sensing parameters could be used, such as the resonance line-width or Q-factor.

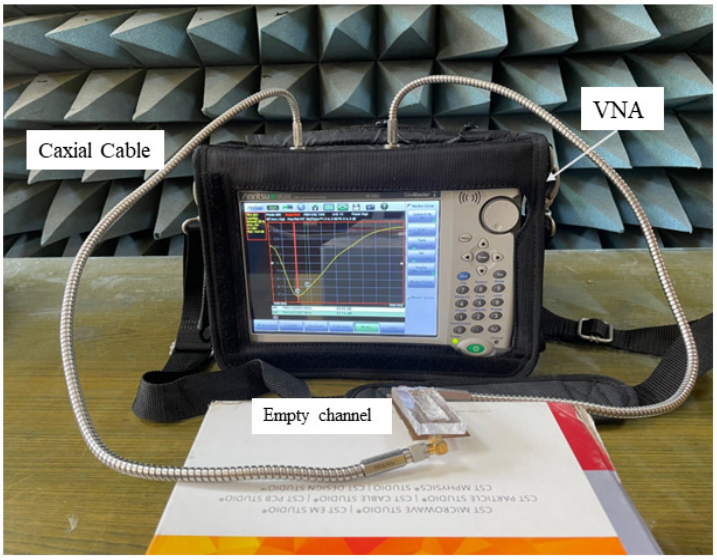

(a)

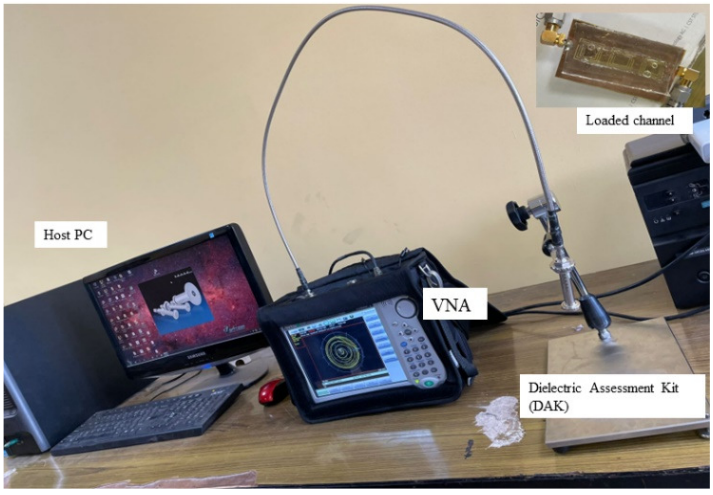

(b)

Figure 6. Complete experimental setup (a) With the help of coaxial cable VNA is connected to a microfluidic sensor. (b) Host PC, VNA, and DAK for dielectric constant measurement of liquids.

Using the Dielectric assessment kit, the VNA has been calibrated for measurement of several liquid types before being utilised to record transmission scattering response. According to Fig. 7, which illustrates the S21 resonance in the unloading stage (blue curve), the plain biosensor has a transmission resonance at 1.6GHz (Red curve). All future liquid sample measurements have been made using PDMS channel and response. The experimental platform contains a micropipette that allows accurate volume over the sensor region at a consistent flow rate when inserting liquid samples into the PDMS channel. All sensing tests have been carried out in a controlled setting to overcome the environmental impact on the collected scattering data and to maintain uniform operating conditions for all the measurements.

B. Measurements using liquid sensing

Three samples, distilled water, Glycerol, and a human tissue mimicking liquid, has been put into the PDMS, placed over the sensor, to investigate its capabilities and sensitivities for distinguishing diverse liquid samples. With different dielectric constants each liquid has different frequency response. Dielectric constants for Distilled Water, Glycerol, and Human Tissue Mimicking Liquid, which have been found through dielectric assessment kit (DAK), and have been depicted in Table 2.
To ensure the stability of the sensing measurements, a liquid sample has been put into the PDMS channel in each measurement trial, and the scattering response of the sensor has been recorded on the VNA. The channel is capable of sensing liquids up to 500µL in volume, although preliminary experiments have demonstrated that the sensor can deliver stable results for low volumes which is 400µL when the loaded liquid is evenly distributed across the sensing surface. A cleaning procedure for the microfluidic channel has been carried out to ensure the capture of independent sensing data from sequential measurements of different liquid samples.

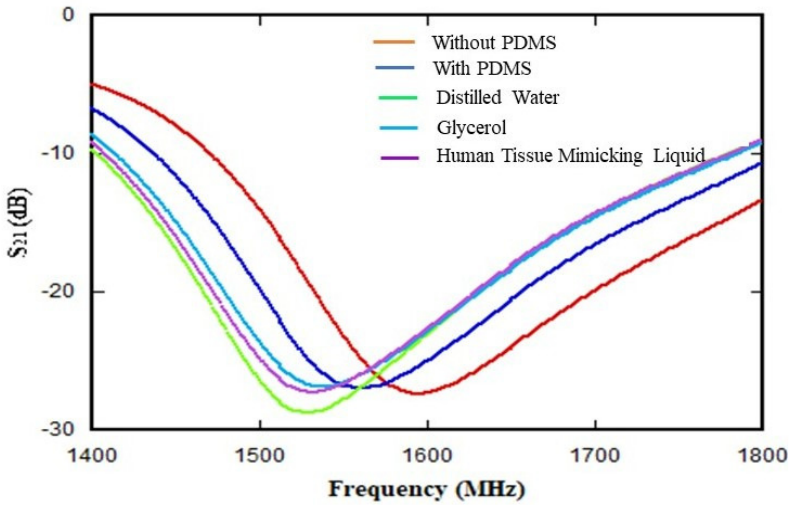

Figure 7. Sensor response curve for different types of liquid.

After each measurement, the tested liquid sample has been flushed out, and pure water has been used to clean the channel, and it has been drained out appropriately. As a result, the pre-loading sensing reference (i.e. base line)
should be retrieved in order to execute the following measurement equitably. The next step has been to fill the PDMS channel with liquid sample and repeat the procedure. Precautions have been taken to avoid the creation of air bubbles inside the PDMS channel, which could affect the sensing measurements. The reflection coefficient (S_{21}) v/s frequency plot for different types of liquids, with successfully resulted different frequency for different kind of liquids with different dielectric constants has been shown in fig. 7, As can be observed, the frequency range for the S_{21} of each liquid is between 1.5 to 1.6 GHz.

Table 2
Dielectric Constant of different liquids:

S. No.	Different liquids	Dielectric constant (ε)
1	Distilled Water	71.0
2	Glycerol	46.5
3	Human tissue Mimicking Liquid	38.0

4. Conclusion

The work presented here introduces a unique, improved microwave microfluidic sensor for liquid detection. To expand the sensing region, the interaction fields, and the sensitivity necessary to detect minute dielectric constants of lossy liquids flowing through the sensing zone inside a PDMS channel, the proposed sensor structure has three cascaded square shaped CSRR cells that are cooperatively coupled. The interaction between loaded liquids inside the channel and the electric field connected to the sensing area, results in a number of resonance modes with frequency changes in the transmission responses and broadband reflection. Practical in-lab tests on liquids that simulate human tissue mimicking liquid, distilled water, and glycerol have been utilised to confirm that the fabricated sensor performs as intended. The advantages of the designed sensor is low-cost and miniaturised size which is greatly assist for the development as portable non-invasive tool for testing in biological fluids, biomedical liquid sensing, or detecting the presence of disease in a particular area of the body.

It has been determined that a highly sensitive microwave sensor can be used for variety of disease detection like cancer monitoring, blood glucose monitoring and blood pressure monitoring by designing, testing, and fabricating the recommended design for the future scope. Researchers can develop a highly effective disease detection-based microwave sensor using thorough literature survey and associated continuous experiments in this field.

6. Acknowledgements

DM acknowledges the Indo-Swedish Collaborative Project, under the Department of Biotechnology, Ministry of Science and Technology, Govt. of India.

7. References

1. A. E. Omer, G. Shaker, S. Safavi-Naeini, K. Ngo, R. M. Shubair, G. Alquié, F. Deshours, and H. Kokabi. "Multiple-cell microfluidic dielectric resonator for liquid sensing applications." *IEEE Sensors Journal* 21, no. 5, 2020: 6094-6104.
2. A. I. Smida, A. J. Alazemi, M. I. Waly, R. Ghayoula and S. Kim, "Wideband Wearable Antenna for Biomedical Telemetry Applications," in IEEE Access, vol. 8, pp. 15687-15694, 2020, doi: 10.1109/ACCESS.2020.2967413.
3. Kayal, Sanchita, Tarakeswar Shaw, and Debasis Mitra. "Design of metamaterial-based compact and highly sensitive microwave liquid sensor." Applied Physics A 126, no. 1 (2020): 1-9.
4. Chuma, Euclides Lourenço, Yuzo Iano, Glauco Fontgalland, and Leonardo Lorenzo Bravo Roger. "Microwave sensor for liquid dielectric characterization based on metamaterial complementary split ring resonator." IEEE Sensors Journal 18, no. 24 (2018): 9978-9983.
5. Omer, Ala Eldin, George Shaker, Safieddin Safavi-Naeini, Georges Alquié, Frédérique Deshours, Hamid Kokabi, and Raed M. Shubair. "Non-invasive real-time monitoring of glucose level using novel microwave biosensor based on triple-pole CSRR." IEEE Transactions on Biomedical Circuits and Systems 14, no. 6 (2020): 1407-1420.
6. Ebrahimi, Amir, Withawat Withayachumnankul, Said Al-Sarawi, and Derek Abbott. "High-sensitivity metamaterial-inspired sensor for microfluidic dielectric characterization." IEEE Sensors Journal 14, no. 5 (2013): 1345-1351.
7. Haq, T., Ruan, C., Zhang, X., Ullah, S., Fahad, A.K. and He, W., 2020. Extremely sensitive microwave sensor for evaluation of dielectric characteristics of low-permittivity materials. Sensors, 20(7), p.1916.
8. Zhang, Xingyun, Cunjun Ruan, Tanveer ul Haq, and Kanglong Chen. "High-sensitivity microwave sensor for liquid characterization using a complementary circular spiral resonator." Sensors 19, no. 4 (2019): 787.
9. Kozak, Ryan, Kasra Khorsand, Telnaz Zarifi, Kevin Golovin, and Mohammad H. Zarifi. "Patch antenna sensor for wireless ice and frost detection." Scientific Reports 11, no. 1 (2021): 1-11.
10. Soffiatti, André, Yuri Max, Sandro G Silva, and Laércio M de Mendonça. "Microwave metamaterial-based sensor for dielectric characterization of liquids." Sensors 18, no. 5 (2018): 1513.
11. Torun, Hamdi, F. Cagri Top, G. Dundar, and A. D. Yalcinkaya. "An antenna-coupled split-ring resonator for biosensing." Journal of Applied Physics 116, no. 12 (2014): 124701.
12. Hofmann, Maximilian, Georg Fischer, Robert Weigel, and Dietmar Kissinger. "Microwave-based noninvasive concentration measurements for biomedical applications." IEEE Transactions on Microwave Theory and Techniques 61, no. 5 (2013): 2195-2204.
13. R. Chandra, H. Zhou, I. Balasingham and R. M. Narayanan, "On the Opportunities and Challenges in Microwave Medical Sensing and Imaging," in IEEE Transactions on Biomedical Engineering, vol. 62, no. 7, pp. 1667-1682, July 2015, doi: 10.1109/TBME.2015.2432137.
14. S. Kiani, P. Rezaei and M. Fakhr, "Dual-Frequency Microwave Resonant Sensor to Detect Noninvasive Glucose-Level Changes Through the Fingertip," in IEEE Transactions on Instrumentation and Measurement, vol. 70, pp. 1-8, 2021, Art no. 6004608, doi: 10.1109/TIM.2021.3052011.
15. Gao, Wei, Sam Emaminejad, Hnin Yin Yin Nyein, Samyuktha Challa, Kevin Chen, Austin Peck, Hossain M. Fahad et al. "Fully integrated wearable sensor arrays for multiplexed in situ perspiration analysis." Nature 529, no. 7587 (2016): 509-514.
16. Mehrotra, Parikha, Baibhab Chatterjee, and Shreyas Sen. "EM-wave biosensors: A review of RF, microwave, mm-wave and optical sensing." Sensors 19, no. 5 (2019): 1013.
17. F. Costa, M. Borgese, M. Degiorgi, and A. Monorchio, “Electromagnetic characterisation of materials by using transmission/reflection (T/R) devices,” Electronics, vol. 6, no. 4, p. 95, Nov. 2017.